Finite Element Modelling of Built-Up CFS Channel Columns Under Axial Load

Krishanu Roy, Tina Chui Huon Ting, Hieng Ho Lau and James B. P. Lim

Abstract A finite element model is described in this paper, which investigates the behaviour of CFS built-up channel columns, connected back-to-back with the help of intermediate web fasteners, subjected to axial load. Finite element package ABAQUS was used to develop the finite element models for built-up columns, which were verified against the test results reported by the authors. Non-linearities of materials and initial imperfections were included in the FEA model. Axial capacity, deformation patterns and load–displacement behaviour were reported from the FE analyses and validated against the test results, reported by the authors in another paper. Axial strengths obtained from the FEA modes were verified against the AISI and AS/NZS design strengths, for CFS built-up columns; obtained comparisons showed that AISI and AS/NZS standards were un-conservative for stub and short columns which failed by local buckling, whereas standards were over-safe for columns failed through overall buckling.

Keywords Cold-formed steel · Back-to-back sections · Built-up columns · Buckling · Fasteners

Notation

A'	Total length of the web
A_e	Effective sectional area

K. Roy (✉) · J. B. P. Lim
Department of Civil and Environmental Engineering,
University of Auckland, Auckland, New Zealand
e-mail: kroy405@aucklanduni.ac.nz

T. C. H. Ting
Faculty of Engineering and Science, Curtin University Malaysia, Miri, Sarawak, Malaysia

H. H. Lau
Faculty of Engineering, Computing and Science, Swinburne University of Technology, Sarawak Campus, Kuching, Sarawak, Malaysia

S. Pulugurtha et al. (eds.), *Advances in Transportation Engineering*,
Lecture Notes in Civil Engineering 34,
https://doi.org/10.1007/978-981-13-7162-2_7

B'	Total flange width
C'	Total lip width
CFS	Cold-formed steel
t	Section thickness
COV	Coefficient of variation
E	Young's modulus
F_n	Critical buckling stress
$(KL/r)_{ms}$	Modified slenderness
$(KL/r)_o$	Overall Slenderness
P_{AISI}	Axial capacity in accordance with American Iron and Steel Institute
P_{FEA}	Axial capacity determined from the finite element investigations
S	Longitudinal spacing between fasteners
λ_c	Non-dimensional slenderness ratio

1 Introduction

The use of CFS built-up channels, connected back-to-back at the webs, is increasing (see Fig. 1), as compression members because of its superior strength-to-self weight ratios and economic design. Cold-formed steel members are easy to construct and also to compare hot-rolled steel members. CFS industry is looking for most effective cross sections of the structural members. However, for large span beam and column members, it is very effective to connect more than one section together to form a built-up section. These built-up sections can carry higher loads and can be used for larger spans, e.g. columns in warehouse or shopping malls, steel trusses, portal frames, space frames and wall frames. Current design guidance according to the American Iron and Steel Institute [1] and the Australian and New Zealand Standards (AS/NZS 4600: 2005) uses modified slenderness method to determine the axial capacity of CFS built-up channels. However, the applicability of the modified slenderness method has not been justified for CFS, unlike hot-rolled steel built-up columns.

Very few researches have been done to determine the axial strength of CFS built-up channel sections, as shown in Fig. 1. The effect of fastener spacing on the strength of built-up channels, connected back-to-back, was investigated by Ting et al. [14] which was followed by Roy et al. [6] to study the effect of thickness on the axial strength of built-up CFS channel sections, connected at the webs of two channels. CFS built-up battened columns were investigated by Dabaon et al. [3], and they have concluded that the AISI and AS/NZS and the eurocodes were un-conservative for columns undergoing local buckling but the standards predicted the failure load safely for those built-up columns failed through flexural buckling. Piyawat et al. [5] investigated welded back-to-back built-up columns. Zhang and Young [19] considered an opening in the CFS built-up columns, connected back-to-back (see Fig. 2). Whittle et al. [18] investigated the axial strengths of built-up columns which were welded toe-to-toe. Stone and LaBoube [16] considered stiffened flange and track back-to-back channel sections. Other works include that of Fratamico et al. [4] and Anbarasu

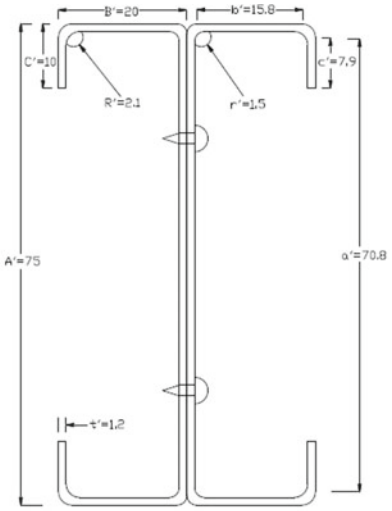

(a) BU75

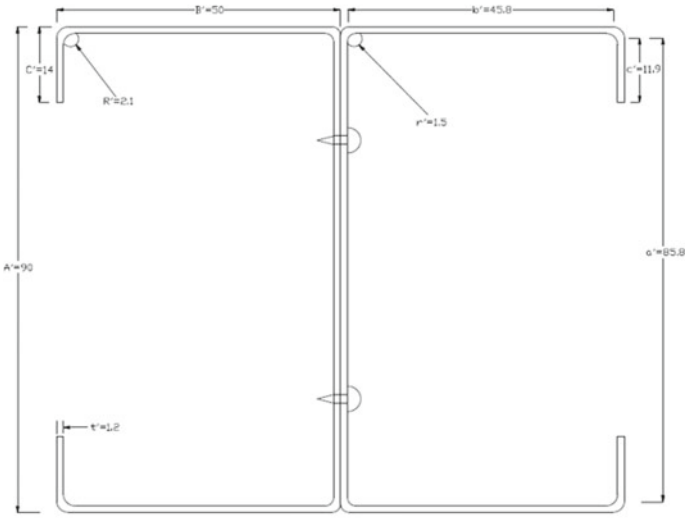

(b) BU90
Dimensions are in mm

Fig. 1 Cross-sectional details of the CFS built-up channel sections investigated herein

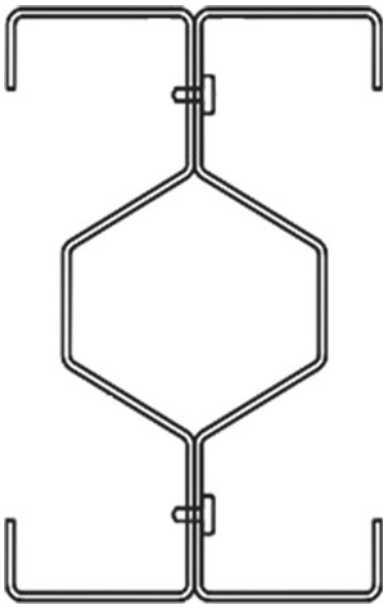

Fig. 2 Built-up CFS section investigated by Zhang and Young [19]

et al. [2] who considered CFS built-up columns, connected back-to-back, while CFS built-up columns, connected by intermediate screws and wood sheathed, were investigated experimentally by Fratamico et al. [4]. On the other hand, Roy et al. [15] investigated the investigated the effect of fastener spacing on axial capacity of built-up duplex stainless steel channels, connected back-to-back. Roy et al. [11–13] also studied experimentally and numerically, the axial capacity of built-up CFS channel sections, connected back-to-back with a gap between two channels and concluded that the current design guidelines by AISI and AS/NZS can be too conservative while predicting the axial capacity of such columns. Also, investigated by Roy et al. [7], the behaviour of built-up CFS un-lipped channel sections, connected back-to-back, subjected to compressive force. The cold-formed built-up stainless steel un-lipped channel sections under compression were investigated by Roy et al. [13]. On the other hand, face-to-face built-up CFS channels were tested under compression by Roy et al. [14]. Roy et al. [17] investigated the behaviour of built-up CFS columns connected back-to-back under axial load and compared the test results against the current design rules as per AISI and AS/NZS.

Sixty finite element results are presented in this paper for CFS built-up channels connected back-to-back under axial load. FE models considered non-linear material properties and initial imperfections. Explicit modelling of intermediate web fasteners has been described. The axial capacity and deformation patterns of CFS built-up columns are reported. FEA results agreed well when compared against the test results, conducted recently by authors [8–10]. FEA results compared against the AISI and AS/NZS strengths. AISI and AS/NZS standards were shown to be safe for all columns

failed through overall buckling; however, the AISI and AS/NZS were un-conservative for all stub and some short columns which failed by local buckling.

2 AISI and AS/NZS Design Guidelines

Finite element strengths were compared against the design strengths calculated in accordance with the AISI and AS/NZS. For built-up CFS columns, the axial strength is calculated according to AISI and AS/NZS as follows:

$$P_{AISI} = A_e F_n \tag{1}$$

The critical buckling stress (F_n) is determined as below:

$$\text{For } \lambda_c \leq 1.5: F_n = (0.658\ \lambda_c^2) F_y \tag{2}$$

$$\text{For } \lambda_c > 1.5,\ F_n = \left(\frac{0.877}{\lambda_c^2}\right) F_y \tag{3}$$

The non-dimensional critical slenderness (λ_c) is calculated using Eq. 4:

$$\lambda_c = \sqrt{\frac{F_y}{F_e}} \tag{4}$$

Modified slenderness ratio was used for all calculations as per Eq. 5.

$$\left(\frac{KL}{r}\right)_{ms} = \sqrt{\left(\frac{KL}{r}\right)^2 + \left(\frac{s}{r_{yc}}\right)^2}; \quad \text{For which} \left(\frac{s}{r_{yc}}\right) \leq 0.5 \left(\frac{KL}{r}\right)_o \tag{5}$$

3 Summary of Experimental Tests

The non-linear FEA models, developed herein, were verified against the test results reported by the authors recently [8–10], (see Fig. 1). The built-up lipped channels were tested under compression for different column lengths starting from stub (length of 300 mm) to slender (length of 2000 mm) columns. Thickness of the CFS channels was 1.2 mm. Figures 1b and 2a show cross-sectional details of the built-up columns, investigated by Roy et al. [8–10], to be referred to as BU75 and BU90, respectively. The measured specimen dimensions are shown in Table 1a, b for BU75 and BU90, respectively. In total, 60 specimens were tested, covering four different column heights: 0.3, 0.5, 1 and 2 m. Types of the built-up section, fastener spacing, nominal specimen length and test specimen number were coded by the specimen

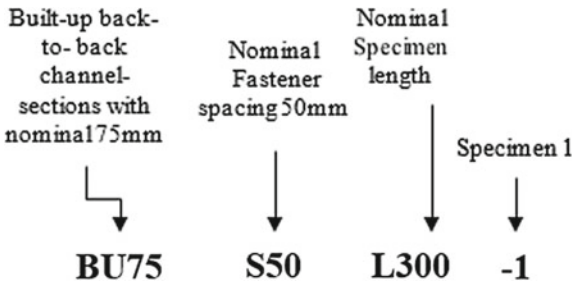

Fig. 3 Specimen labelling

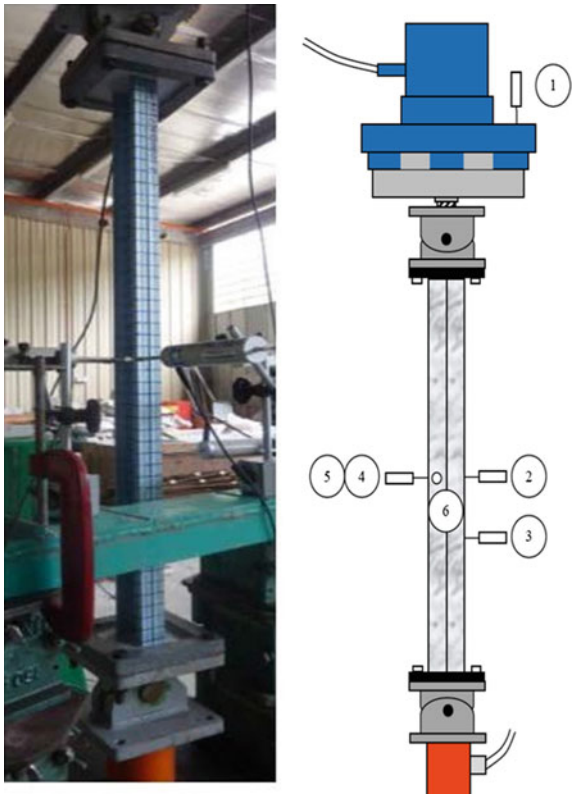

Fig. 4 Built-up column test setup (1-m-long column tests)

labelling. Figure 3 shows an example of the labelling used in the experimental programme.

In order to determine the material properties, i.e. the Young's modulus and yield strength, tensile coupon tests were conducted. From the results of tensile coupon tests for longitudinal and transverse directional coupons, average values of the modulus of elasticity and yield stress were 207 N/mm^2 and 560 N/mm^2, respectively.

All the built-up columns were loaded with the help of a Universal Testing Machine (UTM) (see Fig. 4). The capacity of the UTM was 600 kN. Prior to testing, an LVDT with 0.11 mm accuracy was used to measure initial geometric imperfections present

Table 1 Axial strength comparison from laboratory, finite element analyses and design standards

Specimen	Web	Flange	Lip	Length	Thickness	Spacing	Modified slenderness	Experimental results	AISI design strengths		FEA results	
	A′	B′	C′	L	t	S	$(KL/r)_m$	P_{EXP}	P_{AISI}	P_{Exp}/P_{AISI}	P_{FEA}	P_{Exp}/P_{FEA}
	(mm)	(mm)	(mm)	(mm)	(mm)	(mm)	–	(kN)	(kN)	–	(kN)	–
(a) BU75												
Stub												
BU75S50L300-1	73.1	19.8	11.1	273	1.20	50.0	15.63	120.7	126.68	0.95	116.73	1.09
BU75S50L300-2	73.1	19.8	11.2	280	1.19	50.0	15.93	118.8	126.77	0.94	114.9	1.03
BU75S50L300-3	72.7	19.5	10.8	270	1.21	50.9	15.92	118.7	124.84	0.95	114.4	1.04
BU75S100L300-2	73.1	19.8	11.2	267	1.20	99.7	19.48	117.5	125.10	0.94	113.6	1.03
BU75S100L300-3	73.1	19.9	11.2	273	1.18	100.2	19.41	122.7	125.41	0.98	117.4	1.05
BU75S100L300-4	73.6	19.7	11.2	273	1.18	99.5	19.56	115.4	124.89	0.92	112.6	1.02
BU75S200L300-1	73.7	19.8	11.2	266.5	1.20	200.0	30.31	122.5	119.05	1.03	120.8	1.01
BU75S200L300-2	73.6	19.9	11.2	266	1.20	199.5	30.22	119.1	119.09	1.00	116.4	1.02
BU75S200L300-3	72.9	20.0	11.2	268	1.20	200.0	29.97	113.1	119.36	0.95	108.4	1.04
Mean										0.96		1.04
COV										0.04		0.02
Short												
BU75S100L500-1	73.6	19.8	11.2	655.0	1.21	100.0	69.11	83.0	78.881	1.05	79.5	1.04
BU75S100L500-3	73.6	19.7	11.2	680.0	1.20	100.5	72.16	74.1	78.376	0.95	78.4	0.95
BU75S200L500-1	73.5	19.5	11.3	653.0	1.18	195.0	73.36	86.2	79.992	1.08	80.3	1.07

(continued)

Table 1 (continued)

Specimen	Web	Flange	Lip	Length	Thickness	Spacing	Modified slenderness	Experimental results	AISI design strengths		FEA results	
	A′	B′	C′	L	t	S	*(KL/r)m*	P_{EXP}	P_{AISI}	P_{Exp}/P_{AISI}	P_{FEA}	P_{Exp}/P_{FEA}
	(mm)	(mm)	(mm)	(mm)	(mm)	(mm)	–	(kN)	(kN)	–	(kN)	–
BU75S200L500-2	73.6	19.6	11.3	678.0	1.19	195.0	75.58	88.9	81.406	1.09	82.7	1.07
BU75S200L500-3	73.4	19.7	11.3	680.0	1.21	200.5	75.60	93.6	86.759	1.08	88.1	1.06
BU75S400L500-1	73.6	19.7	11.3	678.0	1.18	400.0	88.74	74.8	72.417	1.03	74.6	1.00
BU75S400L500-2	73.5	19.7	11.3	679.0	1.20	401.0	89.00	80.6	74.336	1.08	76.3	1.06
Mean										1.05		1.04
COV										0.05		0.05
Intermediate												
BU75S225L1000-1	75.3	20.2	10.4	1133	1.21	225.3	121.36	47.0	42.34	1.11	45.7	1.03
BU75S225L1000-2	75.7	19.9	10.4	1131	1.20	225.3	123.71	46.3	41.05	1.13	44.9	1.03
BU75S450L1000-1	75.8	19.9	10.4	1131	1.21	447.0	133.91	50.4	38.98	1.29	42.4	1.19
BU75S450L1000-2	75.6	19.9	10.4	1133	1.18	450.0	135.07	45.0	38.12	1.18	40.12	1.12
BU75S450L1000-3	75.9	19.8	10.3	1182	1.19	450.0	140.52	41.8	34.62	1.21	35.8	1.17
BU75S900L1000-1	76.0	19.9	10.3	1131	1.20	900.0	171.43	39.9	33.21	1.20	34.2	1.17
BU75S900L1000-2	76.3	19.8	9.1	1133	1.21	900.0	178.06	33.7	30.29	1.11	31.5	1.07
BU75S900L1000-3	75.9	19.8	10.3	1183	1.22	901.0	176.55	31.5	28.91	1.09	29.6	1.06
Mean										1.17		1.11
COV										0.07		0.07

(continued)

Table 1 (continued)

Specimen	Web	Flange	Lip	Length	Thickness	Spacing	Modified slenderness	Experimental results	AISI design strengths		FEA results	
	A′	B′	C′	L	t	S	$(KL/r)_m$	P_{EXP}	P_{AISI}	P_{Exp}/P_{AISI}	P_{FEA}	P_{Exp}/P_{FEA}
	(mm)	(mm)	(mm)	(mm)	(mm)	(mm)	–	(kN)	(kN)	–	(kN)	–
Slender												
BU75S475L2000-2	73.9	20.3	10.7	2184	1.20	474.5	231.2	10.9	10.27	1.03	10.6	1.03
BU75S475L2000-3	73.9	20.2	10.8	2183	1.20	462.0	231.61	10.8	10.22	1.03	10.5	1.03
BU75S950L2000-2	73.9	20.3	10.8	2184	1.18	949.5	255.17	8.8	8.43	1.02	8.6	1.02
BU75S950L2000-3	73.9	20.2	10.8	2184	1.17	950.0	256.21	8.6	8.36	1.01	8.5	1.01
BU75S1900L2000-2	73.9	20.3	10.9	2183	1.18	1900.0	334.82	7.6	7.34	1.03	7.4	1.03
BU75S1900L2000-3	73.9	20.4	10.7	2184	1.19	1901.0	333.86	7.5	7.31	1.01	7.4	1.01
Mean										1.02		1.02
COV										0.01		0.01
(b) *BU90*												
Stub												
BU90S50L300-1	91.3	49.8	14.6	277.0	1.20	50.0	7.95	172.5	179.7	0.96	162.7	1.06
BU90S50L300-2	91.8	49.7	14.5	272.0	1.19	49.8	7.89	171.6	182.6	0.94	160.4	1.07
BU90S50L300-3	92.9	49.4	14.5	261.0	1.21	50.0	7.93	170.6	179.6	0.95	160.9	1.06
BU90S100L300-1	90.8	49.7	14.6	262.0	1.20	99.9	9.45	166.2	178.7	0.93	152.5	1.09
BU90S100L300-2	90.6	49.5	14.6	268.0	1.18	100.0	9.42	165.8	176.4	0.94	156.4	1.06

(continued)

Table 1 (continued)

Specimen	Web	Flange	Lip	Length	Thickness	Spacing	Modified slenderness	Experimental results	AISI design strengths		FEA results	
	A′	B′	C′	L	t	S	$(KL/r)_m$	P_{EXP}	P_{AISI}	P_{Exp}/P_{AISI}	P_{FEA}	P_{Exp}/P_{FEA}
	(mm)	(mm)	(mm)	(mm)	(mm)	(mm)	–	(kN)	(kN)	–	(kN)	–
BU90S200L300-1	90.7	49.4	14.6	273.5	1.18	201.0	11.93	163.3	175.6	0.93	157.0	1.04
BU90S200L300-2	90.7	49.4	14.6	269.5	1.20	199.0	11.83	163.5	173.9	0.94	155.7	1.05
BU90S200L300-3	89.5	48.3	14.0	280.5	1.20	199.0	11.87	162.9	173.3	0.94	158.2	1.03
BU90S50L300-1	91.3	49.8	14.6	277.0	1.20	50.0	7.95	172.5	179.7	0.96	162.7	1.06
Mean										0.94		1.06
COV										0.01		0.02
Short												
BU90S100L500-1	90.6	49.5	14.6	656.0	1.21	100.5	35.42	160.4	149.9	1.04	152.8	1.05
BU90S100L500-2	90.6	49.4	14.6	678.0	1.20	100.5	34.25	158.1	152.0	1.08	153.5	1.03
BU90S200L500-1	90.4	49.3	14.7	653.0	1.18	199.5	38.52	152.2	140.9	1.09	142.2	1.07
BU90S200L500-2	90.4	49.3	14.7	678.0	1.19	199.5	39.41	150.9	138.4	1.10	142.4	1.06
BU90S200L500-3	90.4	49.3	14.6	680.0	1.21	200.5	40.20	149.2	135.6	1.06	143.5	1.04
BU90S400L500-1	90.6	49.4	14.7	678.0	1.18	400.0	50.20	132.4	124.9	1.06	127.3	1.04
BU90S400L500-2	90.4	49.4	14.7	678.0	1.20	399.0	49.41	134.5	126.9	1.07	128.1	1.05
Mean										1.07		1.05
COV										0.02		0.01

(continued)

Table 1 (continued)

Specimen	Web	Flange	Lip	Length	Thickness	Spacing	Modified slenderness	Experimental results	AISI design strengths		FEA results	
	A′	B′	C′	L	t	S	$(KL/r)_m$	P_{EXP}	P_{AISI}	P_{Exp}/P_{AISI}	P_{FEA}	P_{Exp}/P_{FEA}
	(mm)	(mm)	(mm)	(mm)	(mm)	(mm)	–	(kN)	(kN)	–	(kN)	–
Intermediate												
BU90S225L1000-1	90.8	49.6	14.4	1182	1.21	225.0	60.42	102.6	92.43	1.11	100.6	1.02
BU90S225L1000-2	90.6	49.6	14.3	1132	1.20	225.0	58.21	102.0	92.72	1.10	99.03	1.03
BU90S450L1000-1	90.6	49.7	14.4	1130	1.21	450.0	64.21	96.51	86.18	1.12	90.20	1.07
BU90S450L1000-2	90.4	49.7	14.4	1182	1.18	448.0	66.21	94.42	82.79	1.14	89.08	1.06
BU90S450L1000-3	90.5	49.8	14.5	1180	1.19	452.0	65.29	93.33	82.54	1.13	87.22	1.07
BU90S900L1000-1	90.5	49.6	14.4	1131	1.20	897.0	75.21	89.55	82.89	1.08	85.29	1.05
BU90S900L1000-2	91.0	49.3	14.4	1182	1.21	899.0	77.21	87.58	80.31	1.09	82.62	1.06
BU90S900L1000-3	90.1	49.2	14.5	1129	1.22	896.0	76.50	87.51	79.51	1.10	84.14	1.04
Mean										1.11		1.05
COV										0.07		0.02
Slender												
BU90S475L2000-1	90.6	49.5	14.5	2164	1.20	474.2	92.52	65.40	61.12	1.07	62.88	1.04
BU90S475L2000-2	90.7	49.4	14.3	2172	1.20	466.6	94.42	66.01	61.63	1.07	62.87	1.05
BU90S950L2000-1	90.5	49.5	14.6	2169	1.18	960.4	101.17	54.02	50.90	1.06	52.45	1.03
BU90S950L2000-2	90.4	49.2	14.5	2148	1.17	949.3	103.21	45.62	43.41	1.05	44.73	1.02

(continued)

Table 1 (continued)

Specimen	Web	Flange	Lip	Length	Thickness	Spacing	Modified slenderness	Experimental results	AISI design strengths		FEA results	
	A′	B′	C′	L	t	S	$(KL/r)_m$	P_{EXP}	P_{AISI}	P_{Exp}/P_{AISI}	P_{FEA}	P_{Exp}/P_{FEA}
	(mm)	(mm)	(mm)	(mm)	(mm)	(mm)	–	(kN)	(kN)	–	(kN)	–
BU90S1900L2000-1	90.5	49.3	14.6	2158	1.18	1902.4	115.2	48.04	44.80	1.07	48.53	0.99
BU90S1900L2000-2	90.9	49.7	14.2	2152	1.19	1906.7	116.42	43.21	41.14	1.05	43.21	1.00
Mean										1.06		1.02
COV										0.02		0.02

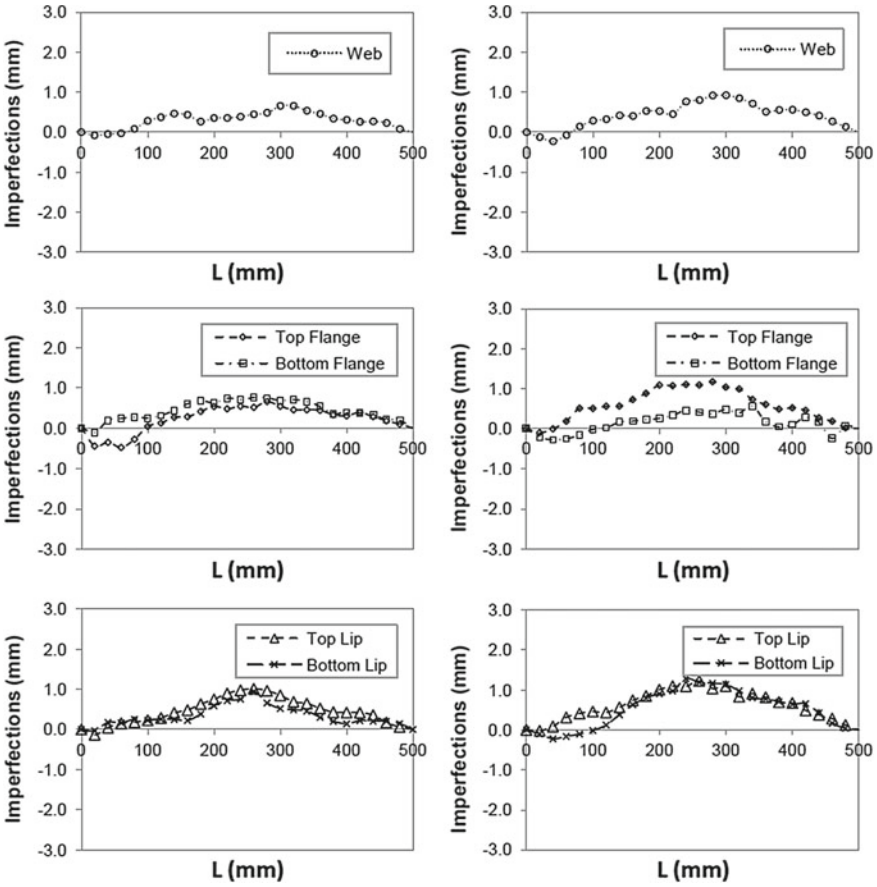

Fig. 5 Initial imperfections for BU90-S200-L300-1

in the channel sections. In Fig. 5, initial imperfections are plotted against the length of the built-up columns for BU90S200L300-1. These imperfections are included in FEA models described in this article. Further details of the experimental tests are available in [8–10].

4 Numerical Study

4.1 General

ABAQUS 6.14-2 was used to develop a finite element model for CFS built-up columns under axial load. Centre line dimensions were used for all FEA models.

Two types of finite element analysis were performed for buckling of built-up sections: Eigenvalue analysis and load–displacement analysis. Eigenvalues of the built-up columns were determined to model the geometric imperfections. A load–displacement non-linear analysis was, then, carried out using RIKS algorithm available in the ABAQUS library. The geometric imperfections and non-linear material properties were included in the FEA model. From this analysis, the failure loads, buckling modes and load–axial shortenings are determined. Specific modelling techniques are described in detail as below.

4.2 Geometry and Material Properties

The built-up channels were modelled considering the full geometry of the columns including web fasteners. Non-linear stress–strain relationships were specified in the finite element model to incorporate the material non-linearity. The non-linear elastic–plastic model was used for modelling the built-up columns in ABAQUS. Yield stress of 560 MPa and ultimate stress of 690 MPa, along with Young's modulus of 207 GPa, were used in finite element modelling.

4.3 Type of Elements and Finite Element Meshing

S4R5 thick shell elements were used to model the built-up columns. S4R5 elements were four-noded quadrilateral thick shell element. Across the length and width, a mesh size of 5 mm $\times$ 5 mm was used for the convergence of the model. A number of elements were confirmed through a mesh sensitivity analysis. An FE mesh is shown in Fig. 6 for BU75-S100-L500-1.

4.4 Modelling of Boundaries and Loading Procedure

Pin–pinned boundaries were applied in all finite element models for built-up columns. Two rigid plates were used at top and bottom ends of the built-up columns to simulate the experimental test results. Pin–pin boundary condition was modelled by applying rotations and displacements to both the end plates through a reference point. The reference point was considered as the CG of the cross section of built-up channels. The reference point was used to apply the load through the upper end plates. Fasteners between two back-to-back channels were modelled using MPC beam connector elements available in the ABAQUS library (see Fig. 7). MPC beam connector elements were assigned a stress of 62.10 MPa to incorporate the stiffness of the fasteners.

4.5 Contact Modelling

"*Surface to surface*" contact was defined as the interaction of the webs of two channels connected back-to-back. The web of one channel was modelled as slave surface, while the web of other channel section was considered as master surface. There was no penetration between the two contact surfaces.

4.6 Geometric Imperfections in FEA Models

Initial imperfections were considered in the FE modelling. Superimpositions of local and global buckling modes were considered for accurate FE analysis. For all built-up columns, eigenvalue analyses were performed. For local buckling, very small channel thickness was considered; however, for global buckling, large channel thickness was used in finite element models. For local and global buckling modes, lowest eigenmode was used in ABAQUS. The imperfections used in the modelling of built-up channels were calibrated to the values measured from experiments by Roy et al. [8–10]. Besides, local imperfection of 0.5% of channel thickness was included in all finite element models as recommended by Roy et al. [7]. In Fig. 8, the contours of local and overall buckling are shown for BU75-S100-L500-1.

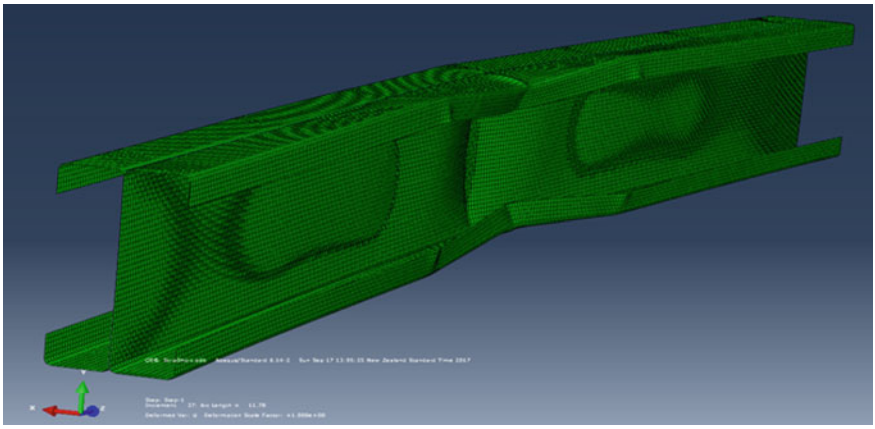

Fig. 6 FE mesh at failure BU75-S100-L500-1

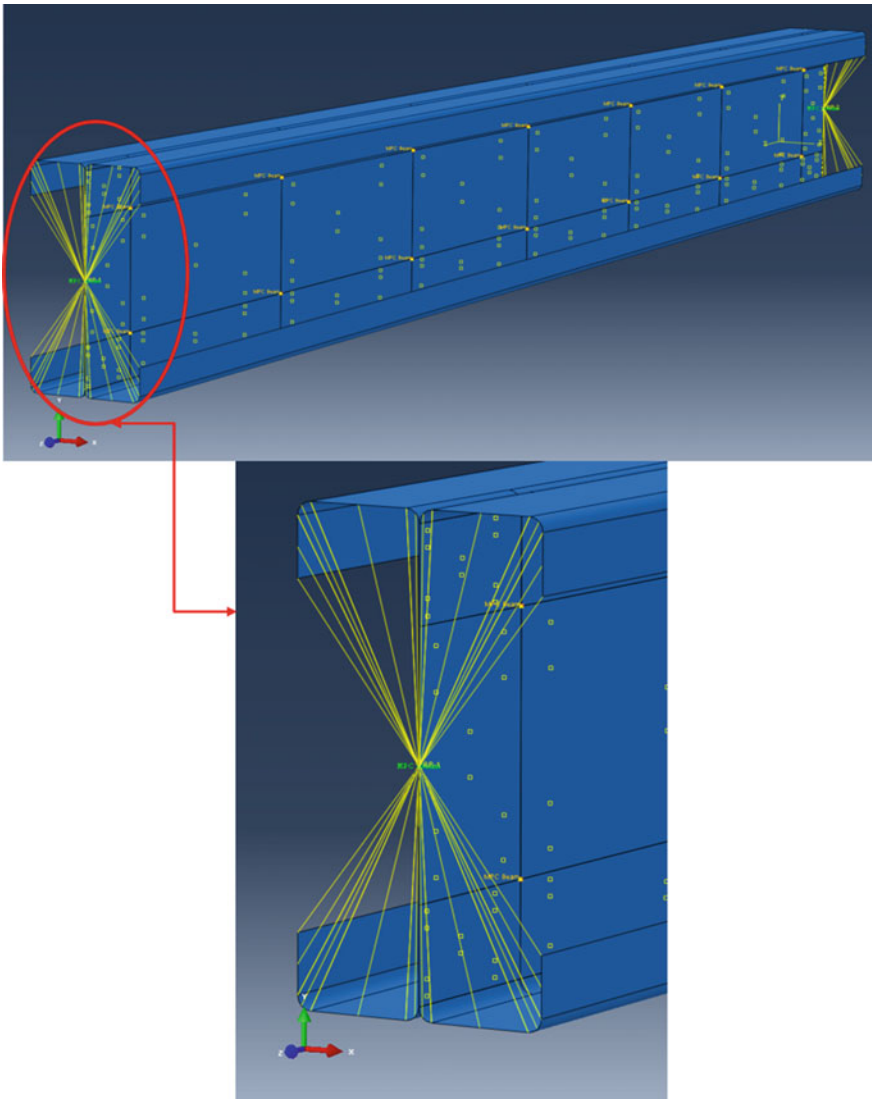

Fig. 7 Boundary condition applied to the FE model (BU75-S100-L500-1)

4.7 FEA Model Validation

Results from the FEA models were verified against the test results available in the literature for built-up CFS columns, connected back-to-back under axial load. Figure 8 shows the failure modes of stub, short and intermediate columns obtained from exper-

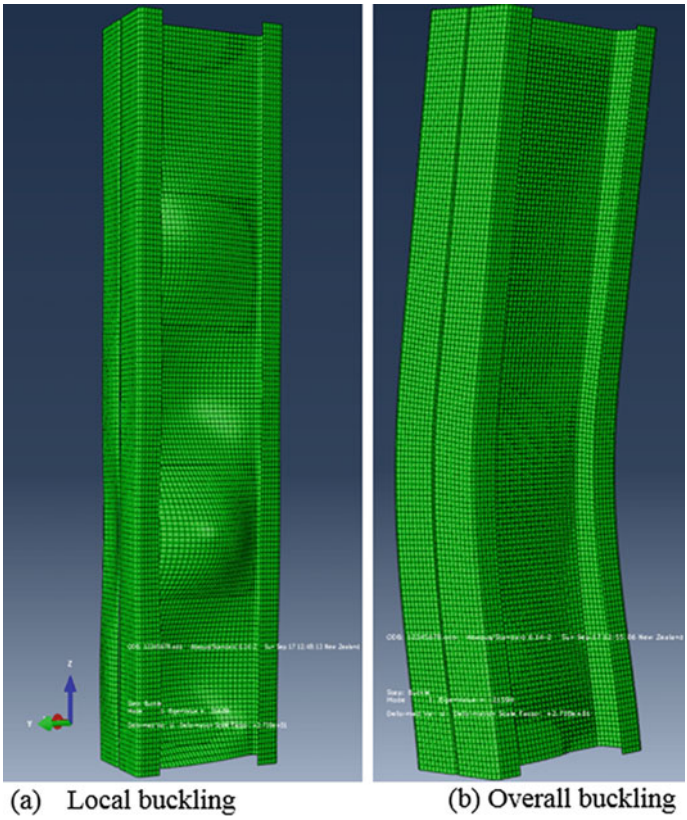

Fig. 8 Initial imperfection contours (BU75-S100-L500-1)

imental tests conducted by Roy et al. [8–10]. Also, in Fig. 9, test and FEA strengths are compared for BU75-S50-L300-1. As can be seen, the tests and FE results show good comparison in terms of both failure load and deformed shapes.

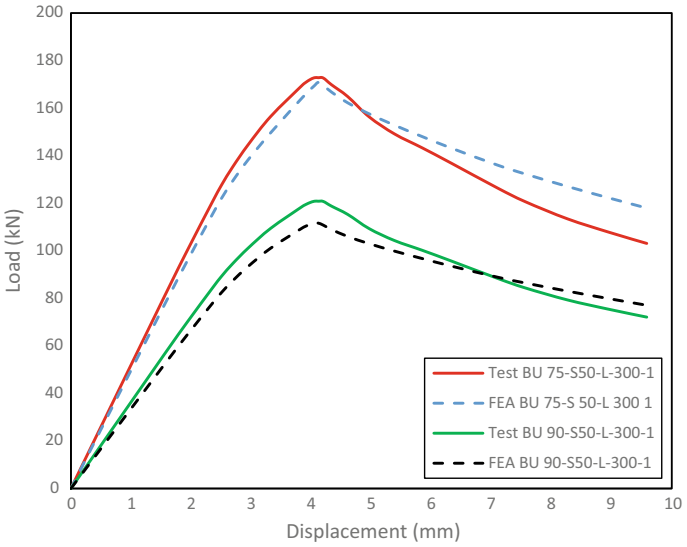

Fig. 9 Comparison of numerical and test results

Table 1a, b summarises the failure load obtained from the tests [8–10], which were compared against the FEA results for BU75 and BU90, respectively. It is shown that the mean of P_{EXP}/P_{FEA} is 1.04, with a COV of 0.02 for stub column of BU75 series and P_{EXP}/P_{FEA} is 1.06, with a COV of 0.02 for stub column of BU90 series.

5 Comparison of FEA Results Against the Design Strengths

Table 1a, b shows the comparison of FEA strengths against the AISI and AS/NZS strengths for BU75 and BU90, respectively. In Table 1a, b, it is shown that the AISI and AS/NZS strengths were higher than FEA strengths by around 10% for all stub columns. For reference, experimental strengths are also included in Table 1a, b for BU75 and BU90, respectively. However, AISI and AS/NZS standard safely predicted the axial capacity of the built-up columns which failed through global or overall buckling.

Figure 11a, b plotted the FEA and design strengths for BU75 and BU90, respectively, against the modified slenderness. Experimental strengths from [8–10] were also plotted in Fig. 11a, b for comparison. It is clear that the FEA strengths are very close to test strengths. From Fig. 10, it can be seen that when the modified slenderness ratio was less than 30, most of the built-up columns failed through local buckling while most of the built-up columns failed through global buckling when the modified slenderness was greater than 55. Comparison of AISI and AS/NZS strengths and FEA strengths are plotted in Fig. 12a, b for BU75 and BU90, respectively.

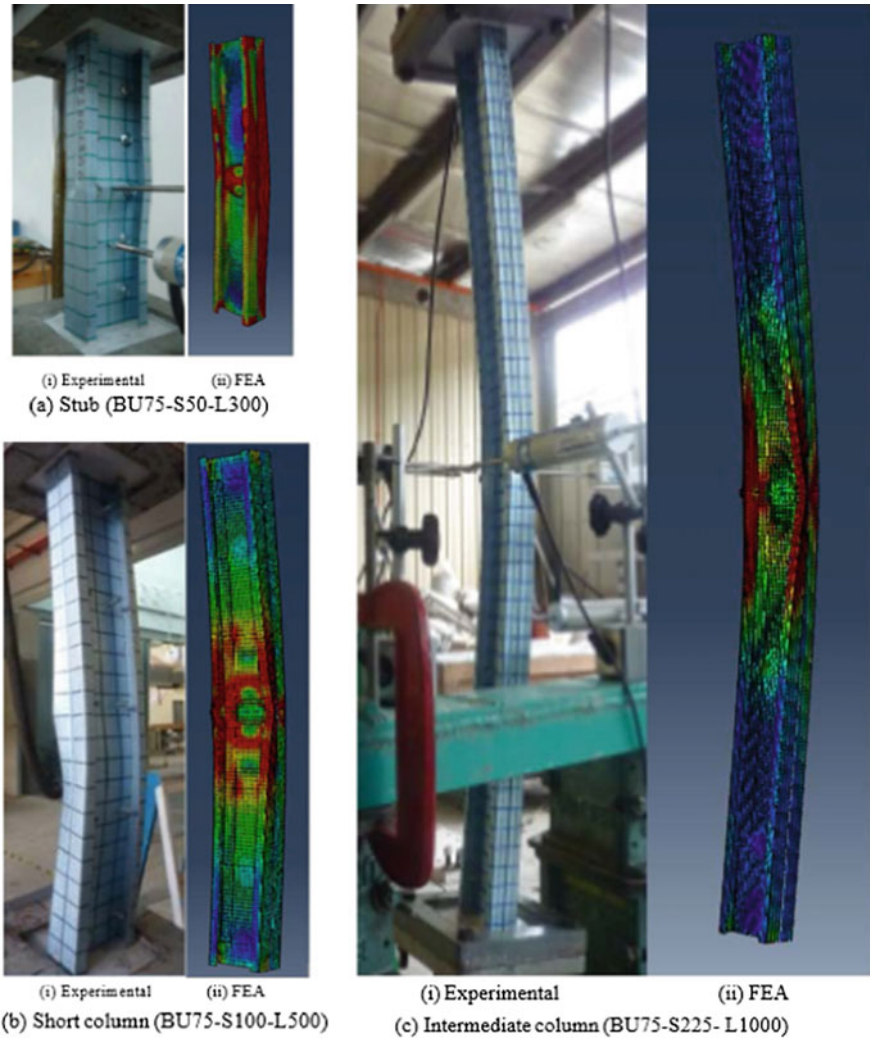

Fig. 10 Built-up sections at failure

6 Conclusions

This paper has presented the results of 60 non-linear FEA analyses on CFS built-up columns, connected back-to-back, subjected to axial load. Finite element model includes explicit modelling of web fasteners, material non-linearity and geometric imperfections. Failure loads and buckling modes for different lengths of built-up columns are discussed. FEA models were validated against the experimental test results which showed good agreement.

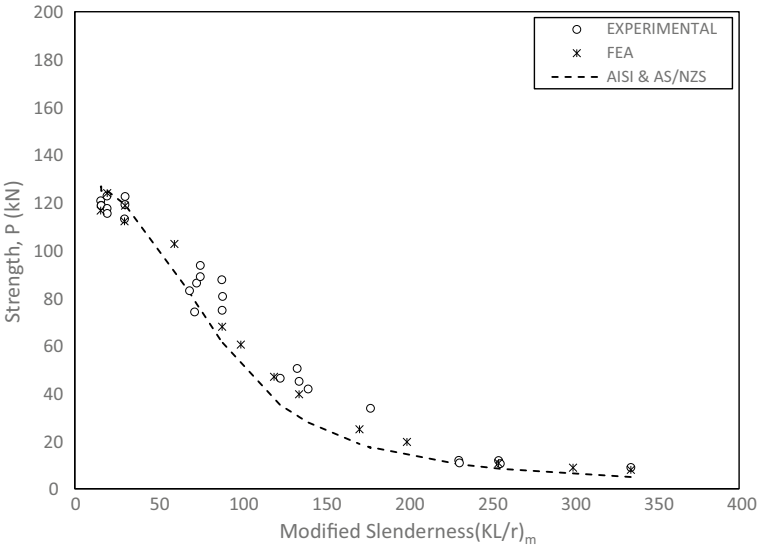

(a)BU75

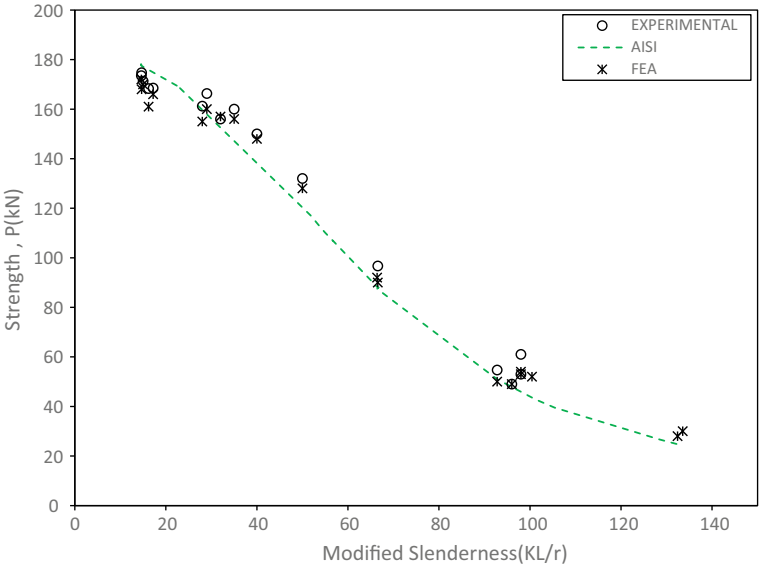

(b)BU90

Fig. 11 Fig. 8: Plot of strength against the modified slenderness

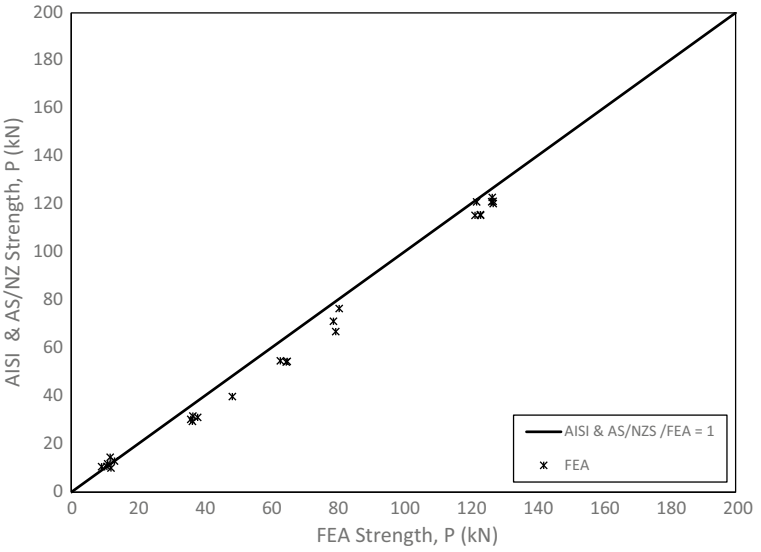

(a) BU75

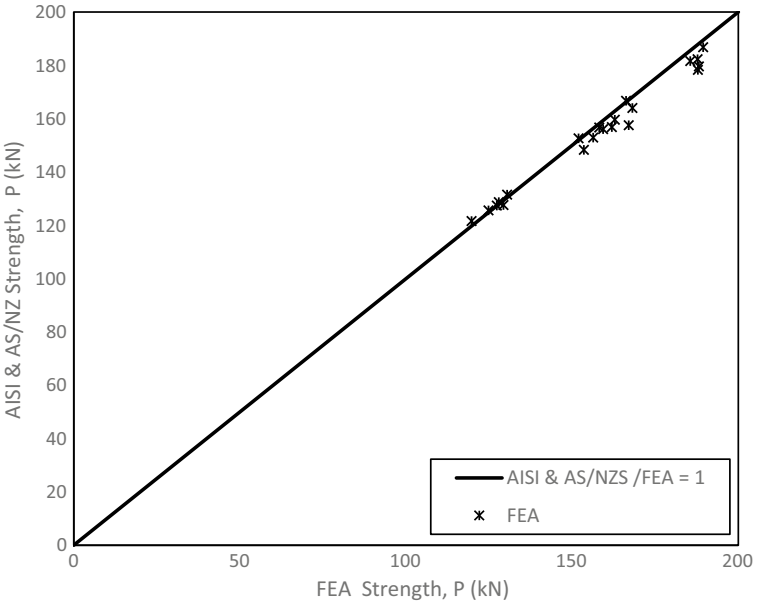

(b) BU90

Fig. 12 FEA strength against the AISI and AS/NZS strengths

The validated FEA models were used to check the accuracy of current design guidelines. The column strengths from the FEA were compared against the AISI and AS/NZS strengths. AISI and AS/NZS strengths were safe by around 15%, when compared to the FEA results for 0.5, 1 and 2 m columns; however, for 0.3 m columns AISI and AS/NZS, they were un-conservative by around 10%.

The first author is currently investigating the effect of different cross sections and arrangement of screws for CFS built-up columns under eccentric load to develop better design methods that will incorporate more accurate estimations of column cross sections and screw spacing for different end conditions.

References

1. American Iron and Steel Institute (2012) North American specification for the design of cold-formed Steel Structural Members. NAS S100
2. Anbarasu M, Bharath KP, Sukumar S (2014) Study on the capacity of cold-formes steel built-up battened colums under axial compression. Lat Am J Solids Struct 11(12):1375–2271
3. Dabaon M, Ellobody E, Ramzy K (2015) Nonlinear behavior of built-up cold-formed steel section battened columns. J Constr Steel Res 110:16–28
4. Fratamico DC, Schafer BW (2014) Numerical studies on the composite action and buckling behavior of built-up cold-formed steel columns. In: 22nd international specialty conference on cold-formed steel structures, St. Louis, MO
5. Piyawat K, Ramseyer C, Kang Thomas H-K (2013) Development of an axial load capacity equation for doubly symmetric built-up cold-formed sections. J Struct Engi Am Soc Civil Eng 139(12):04013008–13
6. Roy K, Lau HH, Lim JBP (2018) Effect of fastener spacing on axial strength of back-to-back built-up cold-formed stainless steel un-lipped channels. Steel Compos Struct Int J
7. Roy K, Mohammadjani C, Lim JBP (2018) Experimental and numerical investigation into the behaviour of face-to-face built-up cold-formed steel channel sections under compression. Thin-Walled Struct (in press)
8. Roy K, Ting TCH, Lau HH, Lim JB (2018) Nonlinear behaviour of back-to-back gapped built-up cold-formed steel channel sections under compression. J Constr Steel Res 147:257–276
9. Roy K, Ting TCH, Lau HH, Lim JBP (2018) Effect of thickness on the behaviour of axially loaded back-to-back cold-formed steel built-up channel sections—experimental and numerical investigation. Structures. https://doi.org/10.1016/j.istruc.2018.09.009
10. Roy K, Ting TCH, Lau HH, Lim JB (2018) Nonlinear behavior of axially loaded back-to-back built-up cold-formed steel un-lipped channel sections. Steel Compos Struct Int J 28(2):233–250
11. Roy K, Ting TCH, Lau HH, Lim JBP (2018) Compression tests on back-to-back gapped built-upcold-formed steel channel sections. In: 2018 Proceedings of the international conference on engineering research and practice for steel construction, ICSC, Hong Kong, China
12. Roy K, Ting TCH, Lau HH, Lim JBP (2018) Effect of screw spacing into the behaviour of back-to-back cold-formed duplex stainless steel built-up channel sections under compression. In: 2018 Proceedings of the international conference on engineering research and practice for steel construction, ICSC, Hong Kong, China
13. Roy K, Ting TCH, Lau HH, Lim JBP (2018) Experimental investigation into the behaviour of back-to-back gapped built-up cold-formed steel channel sections under compression. In: Wei-Wen Yu international specialty conference on cold-formed steel structures, St. Louis, Missouri, USA, 7–8 Nov 2018
14. Roy K, Ting TCH, Lau, HH, Lim JBP (2018) Experimental investigation into the behaviour of CFS built-up channels subjected to axial compression. In: International conference on the

trends and recent advances in civil engineering-TRACE-2018, Noida, Uttar Pradesh, India, 23rd to 24th Aug 2018
15. Standards Australia (2005) Cold-formed steel structures. AS/NZS 4600:2005, Standards Australia/Standards New Zealand
16. Stone TA, LaBoube RA (2005) Behaviour of cold-formed steel built-up I-sections. Thin-Walled Struct 43(12):1805–1817
17. Ting TCH, Roy K, Lau HH, Lim JBP (2018) Effect of screw spacing on behavior of axialy loaded back-to-back cold-formed steel built-up channel sections. Adv Struct Eng 21(3):474–487
18. Whittle J, Ramseyer C (2009) Buckling capacities of axially loaded, cold-formed, built-up channels. Thin-Walled Struct 47(2):190–201
19. Zhang JH, Young B (2012) Compression tests of coldformed steel I-shaped open sections with edge and web stiffeners. Thin-Walled Struct 52:1–11